S. Afr. J. Chem., 2026, 80, S179–S186
https://journals.co.za/content/journal/chem/

Cerium(IV) Decorated Coconut Shell-Reduced Graphene Oxide in Epoxy Resin Matrix as X-Band Radar Absorber Composite

Patricya Inggrid Wilhelmina Bolilanga[1], Rahmat Basuki[1]*, Nugroho Adi Sasongko[2,3,4], Yusuf Bramastya Apriliyanto[1], Arief Budi Santiko[5] and Gunaryo Gunaryo[1]

[1]*Department of Chemistry, Republic of Indonesia Defense University, Bogor, Indonesia*
[2]*Research Center for Sustainable Production System and Life Cycle Assessment, National Research and Innovation Agency (BRIN), Banten, Indonesia*
[3]*Energy Security Graduate Program, The Republic of Indonesia Defense University Bogor, Indonesia*
[4]*Murdoch University, Murdoch, Western Australia, Australia*
[5]*Research Center for Telecommunication, National Research and Innovation Agency (BRIN), Bandung, Indonesia*

ABSTRACT

The development of lightweight and efficient radar-absorbing materials (RAM) remains a critical challenge for electromagnetic (EM) attenuation in modern stealth applications. In this study, a cerium(IV) oxide (CeO_2)-decorated, coconut shell-derived reduced graphene oxide composite embedded in an epoxy matrix (cs-rGO/CeO_2/epoxy) was successfully synthesized using a modified Hummers method followed by hydrothermal reduction. The use of biomass-derived carbon offers a sustainable and low-cost alternative to conventional precursors. Structural and morphological analyses by SEM-EDX, Raman, XRD, and FT-IR instrument confirmed the successful reduction of graphene oxide, the formation of CeO_2 nanoparticles, and their uniform dispersion within the matrix, with an average particle size of 15.38 nm. Electromagnetic measurements revealed a maximum reflection loss (RL) of −7.72 dB at 9.77 GHz in the X-band at a thickness of 1 mm. This performance is attributed to the combined effects of dielectric loss, interfacial polarization, and multiple scattering within the heterogeneous structure. Although the absorption performance remains moderate, the ability of the composite to achieve effective attenuation at low thickness demonstrates its strong potential as a lightweight RAM. The favourable combination of reduced thickness, lightweight characteristics, and microwave attenuation capability makes this composite a promising candidate for advanced electromagnetic wave absorption applications and merits further comprehensive investigation.

KEYWORDS

reduced graphene oxide, coconut shell, cerium(IV) oxide, epoxy resin, radar absorbing material

Received: 1 September 2025 Revised: 21 April 2026 Accepted: 1 June 2026

INTRODUCTION

The development of radar-absorbing materials (RAM) has attracted increasing attention due to their importance in electromagnetic (EM) wave attenuation and stealth technology applications.[1–2] RAMs are designed to minimize reflection while enhancing the absorption of incident EM waves through impedance matching and energy dissipation mechanisms, typically converting EM energy into heat.[3–4] The prototype model of RAM, consisting of carbon and titanium oxide (TiO_2), was first utilized in Germany.[5] However, recent advances in nanostructured materials, including carbon nanotubes, graphene-based materials, and polymer nanocomposites, have significantly improved microwave absorption performance.[6] Ruiz-Perez et al.[4] reported that carbon-based materials are particularly attractive due to their lightweight nature, high electrical conductivity, chemical stability, and tunable dielectric properties. Reduced graphene oxide (rGO), in particular, has demonstrated strong potential as an EM absorber owing to its unique electronic structure and large surface area.[4,6–8]

rGO is commonly synthesized via a modified Hummers method followed by reduction processes such as hydrothermal treatment, producing materials with enhanced electrical and structural properties.[9–13] However, the use of biomass-derived precursors, such as coconut shell, for rGO synthesis remains relatively underexplored despite the advantages of such materials in terms of sustainability, low cost, and waste management. To further enhance EM absorption performance, rGO is often combined with secondary materials such as metals, ferrites, or metal oxides to improve dielectric and magnetic loss mechanisms.[7,14] Surface modification of rGO with these materials can significantly improve EM absorption. Additionally, such modifications can help balance the electrical conductivity of rGO.[13] Therefore, cerium(IV) oxide (CeO_2), with its high dielectric constant and chemical stability, is a promising candidate for such modification.[7,15]

Although graphene-based RAMs have been extensively investigated, most reported systems rely on non-renewable graphite precursors and require relatively thick configurations (typically >2 mm) to achieve effective microwave absorption. The development of sustainable, biomass-derived reduced graphene oxide (rGO) combined with functional metal oxides in thin absorber configurations remains limited. In particular, achieving measurable electromagnetic attenuation at a thickness as low as 1 mm remains a significant challenge. Moreover, studies on the integration of cerium(IV) oxide (CeO_2) into biomass-derived rGO-based polymer composites for thin, lightweight microwave absorbers remain scarce. Therefore, this study aims to develop a cerium(IV)-decorated coconut shell-derived rGO composite dispersed in an epoxy matrix and to systematically investigate its structural, morphological, and electromagnetic properties, with a focus on its microwave absorption performance in the X-band at a thickness of 1 mm.

MATERIALS AND METHODS

Materials

All chemicals (hydrofluoric acid, HF 48%; hydrochloric acid, HCl 37%; sulfuric acid, H_2SO_4 98%; sodium nitrate, $NaNO_3$; potassium permanganate, $KMnO_4$; hydrogen peroxide, H_2O_2 30%; cerium(III) nitrate, $Ce(NO_3)_3$; ammonium hydroxide, NH_4OH 25%; and ethanol, C_2H_5OH) were of analytical grade and supplied by Merck®, Germany, and were used without further purification. Coconut shells were obtained

*To whom correspondence should be addressed
Email: rhmtbsq@gmail.com

ISSN 1996-840X Online / South African Chemical Institute / http://saci.co.za/journal
© The Author(s) Published under a Creative Commons Attribution 4.0 International Licence (CC BY 4.0)
https://doi.org/10.17159/0379-4350/2026/v80se1a18

from Poso, Central Sulawesi. Epoxy resin (Dextone) and hardener Hybrid 951 (HY 951, Dextone) were used as the composite matrix. HY 951 is a low-viscosity hardener suitable for casting applications.

Instrumentation

Fourier transform infrared spectroscopy (FT-IR, Bruker Tensor 27) was used for functional group analysis. The measurements were carried out using the transmission method in the range of 600–4000 cm^{-1} at 25°C using KBr pellets. Scanning electron microscopy coupled with energy-dispersive X-ray spectroscopy (SEM–EDX, JEOL JSM-6390), at an accelerating voltage of 10 kV), was utilized to investigate the surface morphology and chemical composition of the material. Raman shifts were recorded using DXR™3xi Raman Imaging Microscope (Thermo Fisher Scientific) over the range 300–3000 cm^{-1}. X-ray diffraction (XRD, Surveymeter Ranger S/N R309523) analysis was performed using Cu Kα radiation (λ = 1.54 Å) at 40 kV and 30 mA, with a scanning range of 10–79.98° (2° min^{-1}). Electromagnetic absorption properties were evaluated using a vector network analyzer (VNA) in the X-band frequency range (8–12 GHz).

Synthesis of coconut shell-based graphite (cs-Gi)

Coconut shell-based graphite (cs-Gi) was synthesized via a carbonization method following previously reported procedures with slight modifications.[16–18] Coconut shell samples were sieved to 100 mesh and calcined at 200°C for 1 hour. Higher calcination temperatures may induce structural degradation, affecting subsequent processing. This approach is consistent with previous studies.[16] A total of 10 g of the resulting powder was mixed with 30 mL of 40% HF and stirred for 3 hours at 45°C. The mixture was then filtered and washed with 30 mL of 20% HCl under the same conditions. Subsequently, the sample was rinsed with distilled water until neutral pH (pH = 7) was achieved. The material was dried in an oven at 110°C for 12 hours and labeled as cs-Gi. The sample was characterized using SEM–EDX, XRD, and FT-IR.

Synthesis of coconut shell-based graphite oxide (cs-GiO)

Graphite oxide (cs-GiO) was synthesized using a modified Hummers method following Sujiono et al.[15] Briefly, 50 mL of 98% H_2SO_4, 2.0 g of cs-Gi, and 0.5 g of $NaNO_3$ were mixed and stirred for 30 minutes at 50°C. Subsequently, 6.0 g of $KMnO_4$ was gradually added, and the mixture was stirred for 3 hours at a constant temperature. Then, 100 mL of distilled water was added, followed by an additional 200 mL of distilled water while maintaining the same conditions. After 1 hour, 10 mL of 30% H_2O_2 was added and stirred for 30 minutes at 50°C. The mixture was filtered using a vacuum Büchner funnel. The resulting solid was washed with 80 mL of 20% HCl, followed by distilled water until neutral pH (pH = 7) was achieved. The product was dried at 110°C for 12 hours and labeled as cs-GiO. Characterization was performed using SEM–EDX, Raman, XRD, and FT-IR.

Synthesis of cs-rGO/CeO_2/epoxy composite

The cs-rGO/CeO_2 composite was synthesized via one-pot hydrothermal reduction following Wang et al.[16] and Yin et al.[13] Initially, 1.0 g of cs-GiO was dispersed in 60 mL of deionized water and sonicated (200 W, 40 kHz) for 3 hours. Subsequently, 2.52 g of $Ce(NO_3)_3$ was added under magnetic stirring for 1 hour at 25°C. A 25% NH_4OH solution was then added dropwise as a reducing agent until the pH reached 10. The mixture was transferred into a 100 mL Teflon-lined stainless-steel autoclave and heated at 200°C for 12 hours. After cooling, the product was filtered and washed with ethanol and deionized water until neutral pH was achieved. The solid was dried at 110°C for 12 hours. Pure cs-rGO and CeO_2 were prepared using similar procedures. All samples were characterized using SEM–EDX, Raman, XRD, and FT-IR.

For composite fabrication, cs-rGO/CeO_2 powder was dispersed into the epoxy matrix following Ahmad et al.[14] A mixture of 4.0 g (80 wt%) epoxy resin, 0.5 g (10 wt%) cs-rGO/CeO_2, and 0.5 g (10 wt%) hardener (HY 951) was homogenized using a vortex mixer. The mixture was poured into silicone molds with a thickness of 1 mm and cured at 80°C for 12 hours. The resulting composites were characterized using SEM–EDX, XRD, and FTIR.

Characterization

The crystal size (D) and interplanar spacing (d-spacing) were calculated using Debye-Scherrer equation (equation 1) and Bragg's Law (equation 2). K is the dimensionless shape factor, typically approximated as 0.9, λ is the wavelength of Cu K_α radiation, B is full width half maximum (FWHM), n is an order, and θ is Bragg's angle.

$$D = \frac{K.\lambda}{B.\cos\theta} \quad (1)$$

$$d = \frac{n.\lambda}{2.\sin\theta} \quad (2)$$

The reflection coefficient (Γ) was calculated using equation 3. The reflected power and through power value were calculated using the equation 4 and equation 5, respectively.

$$\tilde{A} = 10^{\left(\frac{-\text{Return Loss}}{20}\right)} \quad (3)$$

$$\text{Reflected Power} = 100 \times \Gamma^2 \quad (4)$$

$$\text{Through Power} = 100 \times (1 - \Gamma^2) \quad (5)$$

RESULTS AND DISCUSSION

Characterization of cs-rGO/CeO_2/epoxy

The surface morphology of cs-rGO and its modified composites was examined using SEM (Figure 1–3). The cs-rGO sample exhibits a characteristic wrinkled and layered structure with minimal agglomeration, indicating successful exfoliation during the reduction process.[19] These wrinkles arise from the intrinsic flexibility of graphene sheets and contribute to an increased specific surface area, which enhances electromagnetic (EM) wave interaction.[10,14]

After CeO_2 decoration, a noticeable increase in surface roughness is observed (Figure 2). This result confirms the successful deposition of CeO_2 nanoparticles onto the rGO sheets, forming heterogeneous interfaces, consistent with previous reports.[16] Such interfaces promote interfacial polarization, which contributes to dielectric loss during EM wave absorption. In addition, nanoscale CeO_2 particles introduce multiple scattering pathways, further enhancing EM wave attenuation.[13]

The cs-rGO/CeO_2 particles are uniformly dispersed within the epoxy matrix (Figure 3), with no significant agglomeration observed. This homogeneous distribution indicates good interfacial compatibility between the filler and the polymer matrix.[20–22] Uniform dispersion is essential for achieving effective impedance matching, as it ensures a balanced distribution of conductive and dielectric components throughout the composite. Poor dispersion typically results in localized conductivity and increased reflection,[14] therefore, the observed morphology is expected to improve microwave absorption performance.

Overall, the morphological characteristics indicate that the incorporation of CeO_2 and its subsequent dispersion in the epoxy matrix modify the surface structure and introduce features that may contribute to improved EM wave attenuation.

The elemental composition of cs-rGO and its composites was analyzed using energy-dispersive X-ray spectroscopy (EDX) (Table 1). The cs-rGO sample primarily consists of carbon (83.31%) and oxygen

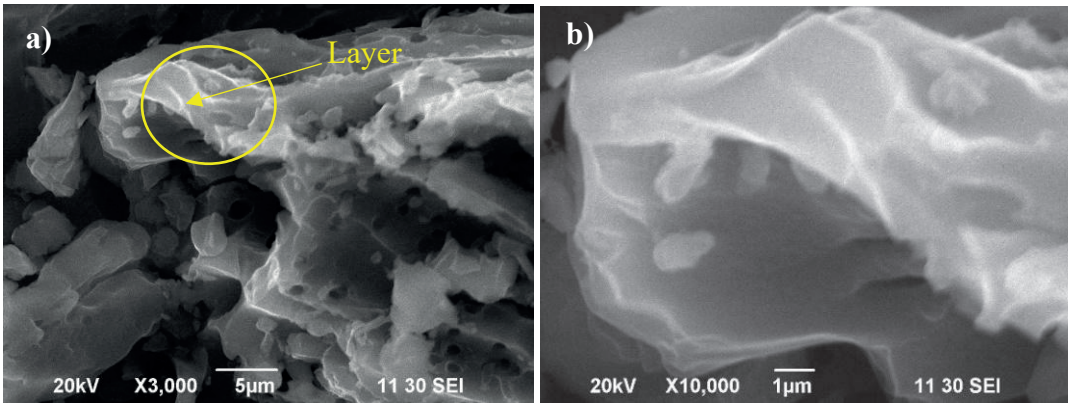


Figure 1: SEM of cs-rGO at 3000× (a) and 10000× (b) magnification.

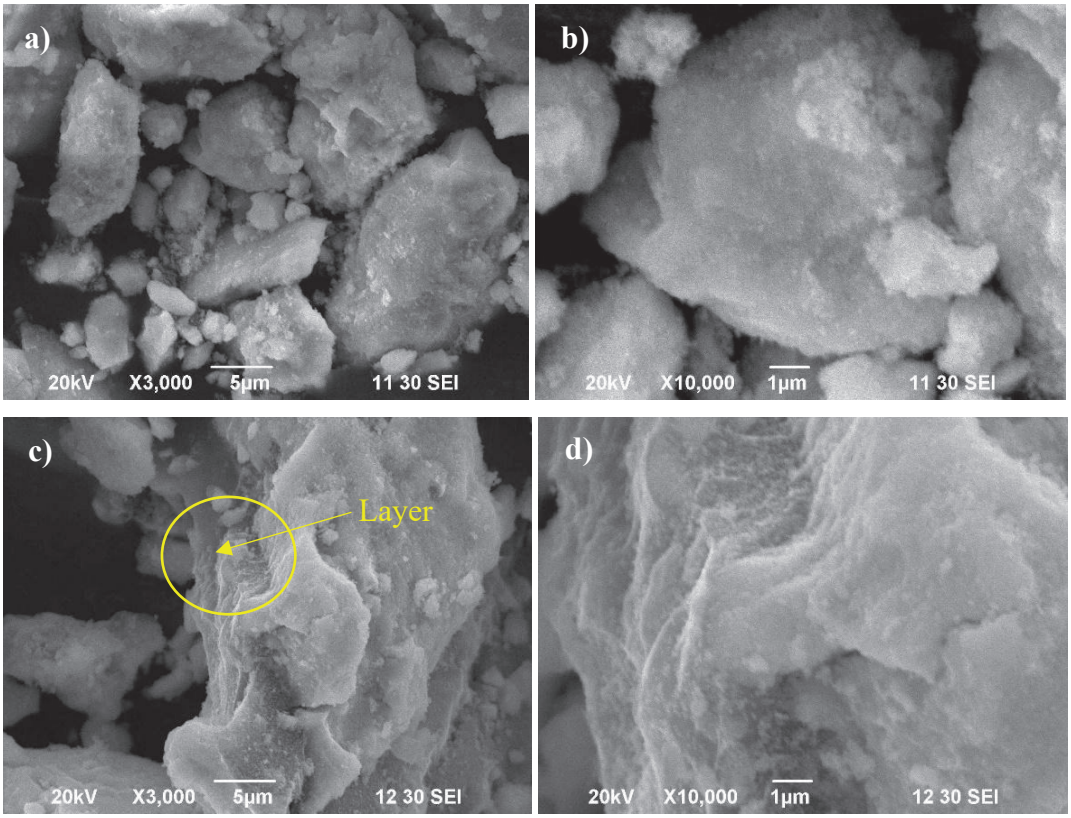


Figure 2: SEM of (a) CeO_2, (c) cs-rGO/CeO_2 at 3000× magnification, (b) CeO_2, and (d) cs-rGO/CeO_2 at 10000× magnification.

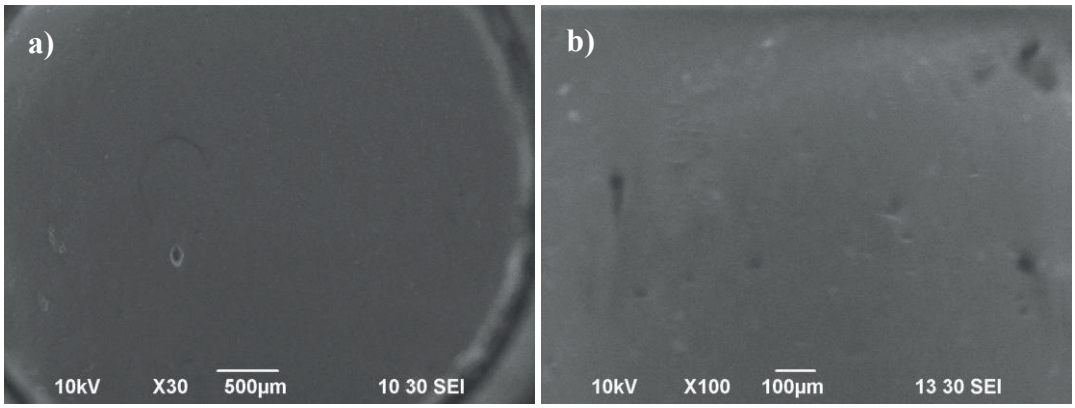


Figure 3: SEM of cs-rGO/CeO_2/epoxy at 30× (a) and 100× (b) magnification.

Table 1: Chemical composition of all samples based on the EDX results

Sample	Element	Line	Weight (%)	Atom (%)	C/O Ratio
cs-rGO	C	K	83.31	86.93	6.65
	O	K	16.69	13.07	
	Total		100.0	100.0	
cs-rGO/CeO_2	C	K	75.32	41.45	3.22
	O	K	17.56	12.87	
	Ce	L	7.11	45.67	
	Total		99.9	99.9	
cs-rGO/CeO_2/ epoxy	C	K	77.57	82.23	4.63
	O	K	22.32	17.76	
	Ce	L	0.11	0.01	
	Total		100.0	100.0	

(16.69%), with a C/O ratio of 6.65. This relatively high ratio indicates effective reduction of oxygen-containing functional groups and partial restoration of the sp^2 carbon network.[22]

After CeO_2 incorporation, the cs-rGO/CeO_2 composite shows the presence of cerium (7.11%), along with carbon (75.32%) and oxygen (17.56%). The detection of cerium confirms the successful integration of CeO_2 into the rGO structure, consistent with previous studies.[22] The decrease in carbon content accompanied by the increase in oxygen content can be attributed to the reconstruction of sp^2 carbon domains and the oxygen contribution from the CeO_2 phase, strongly indicating the effectively formation of the hybrid composite structure. This finding is further corroborated by the Raman analysis.

For the cs-rGO/CeO_2/epoxy composite, carbon (77.57%), oxygen (22.32%), and a lower cerium content (0.11%) were detected. The reduced cerium signal is likely due to dilution by the epoxy matrix and embedding of the filler within the polymer, which limits surface detection.[13–14,22] Nevertheless, the presence of cerium confirms that the functional filler is retained after composite formation.

Raman spectroscopy was performed to evaluate the structural disorder and graphitic characteristics of cs-GiO, cs-rGO, and cs-rGO/CeO_2. As shown in Figure 4, all samples exhibit the characteristic D band (1352–1355 cm^{-1}) and G band (1582–1590 cm^{-1}), corresponding to defect-induced vibration and sp^2 carbon domains, respectively.[23–24] The cs-GiO sample shows a relatively intense D band due to the formation of oxygen-containing functional groups during the Hummers oxidation process. After hydrothermal reduction, the G band shifted from 1590 to 1582 cm^{-1}, indicating the partial restoration of the sp^2 carbon network and successful reduction of graphene oxide.[10] For cs-rGO/CeO_2 sample, the Raman peak observed at approximately 450 cm^{-1} is attributed to the F_{2g} vibrational mode of CeO_2 suggesting the successful incorporation of CeO_2 nanoparticles onto the cs-rGO sheets, in agreement with previous studies.[13,16]

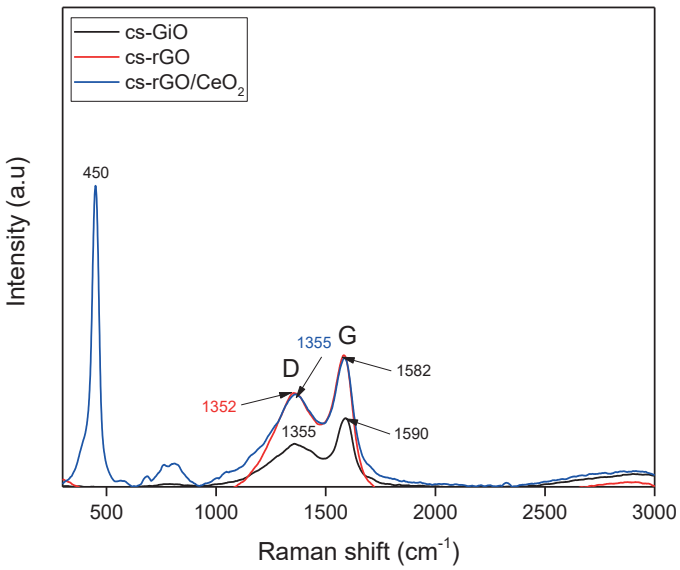


Figure 4: Raman Spectra of cs-GiO, cs-rGO, and cs-rGO/CeO_2

The calculated I_D/I_G ratios for cs-GiO, cs-rGO, and cs-rGO/CeO_2 were 0.617, 0.715, and 0.713, respectively. The increased I_D/I_G ratio after reduction indicates the formation of smaller sp^2 domains and additional defect sites following the removal of oxygen functionalities, which is a typical characteristic of reduced graphene oxide[11,.25] Meanwhile, the nearly unchanged I_D/I_G value of cs-rGO/CeO_2 indicates that CeO_2 decoration did not significantly disrupt the graphitic structure of cs-rGO. The preserved defect sites and sp^2 domains are beneficial for interfacial polarization and dielectric loss, thereby enhancing microwave absorption performance.[7,8]

The crystallinity of the synthesized materials was analyzed using X-ray diffraction (XRD) (Figure 5–6). The cs-Gi, cs-GiO, and cs-rGO samples exhibit broad diffraction peaks at approximately 2θ = 23.74°, 23.51°, and 23.99°, respectively, consistent with JCPDS data (No. 75-2078).[19] These broad peaks indicate predominantly amorphous carbon structures, typical of biomass-derived materials such as coconut shell.[26] During oxidation (cs-Gi to cs-GiO), a slight peak shift and increased interlayer spacing are observed, attributed to the intercalation of oxygen-containing functional groups introduced during the modified Hummers method.[14] After hydrothermal reduction, the cs-rGO sample shows partial restoration of the graphitic structure, indicated by peak shifting and reduced interlayer spacing.[22]

Following CeO_2 incorporation (Figure 5b), distinct diffraction peaks appear at 2θ = 28.71°, 33.26°, 47.75°, and 56.65°, corresponding to the (111), (200), (202), and (311) planes of cubic fluorite CeO_2 (JCPDS No. 34-0394).[8,21] These peaks confirm the formation of crystalline CeO_2 nanoparticles on the rGO surface. The coexistence of amorphous carbon and crystalline CeO_2 indicates a heterogeneous composite structure.

In the cs-rGO/CeO_2/epoxy composite (Figure 6), the characteristic CeO_2 peaks are retained, while an additional broad peak at approximately 2θ = 17.70° corresponds to the amorphous epoxy matrix. This confirms that the crystalline structure of CeO_2 remains stable after composite formation.[8,21] The combination of amorphous carbon and crystalline CeO_2 is beneficial for EM wave absorption, as it enhances dielectric loss and interfacial polarization, improving impedance matching and attenuation efficiency.[14]

Crystallite size (D) and interlayer spacing (d-spacing) values are summarized in Table 2. The cs-Gi, cs-GiO, and cs-rGO samples exhibit relatively small crystallite sizes, consistent with their amorphous structure.[23] An increase in d-spacing during oxidation is observed due to the intercalation of oxygen functional groups introduced by $KMnO_4$ and H_2SO_4.[21,24–25] After reduction, the d-spacing decreases, indicating partial removal of oxygen groups and restacking of graphene layers.[27] The cs-rGO/CeO_2 composite exhibits a crystallite size of 14.50 nm and a d-spacing of 0.256 nm. After incorporation into the epoxy matrix, the crystallite size slightly increases to 15.38 nm, while the d-spacing remains nearly constant (~0.25 nm). This suggests that the structural framework of rGO is preserved during composite formation.[14,28]

Crystallinity analysis shows that cs-rGO has relatively low crystallinity (24.90%), reflecting its disordered structure.[11,28–29] The crystallinity increases significantly in cs-rGO/CeO_2 (69.35%) due to the presence of crystalline CeO_2.[8,30–31] However, after dispersion in the epoxy matrix, the crystallinity decreases to 26.88%, indicating the dominant amorphous nature of the polymer and uniform filler distribution. This reduction suggests the formation of a heterogeneous system containing both crystalline and amorphous phases.[29–30]

Fourier transform infrared (FT-IR) spectroscopy was used to analyze functional group evolution (Figure 7, Table 3). The spectra of cs-Gi, cs-GiO, and cs-rGO (Figure 7a) show characteristic C=C

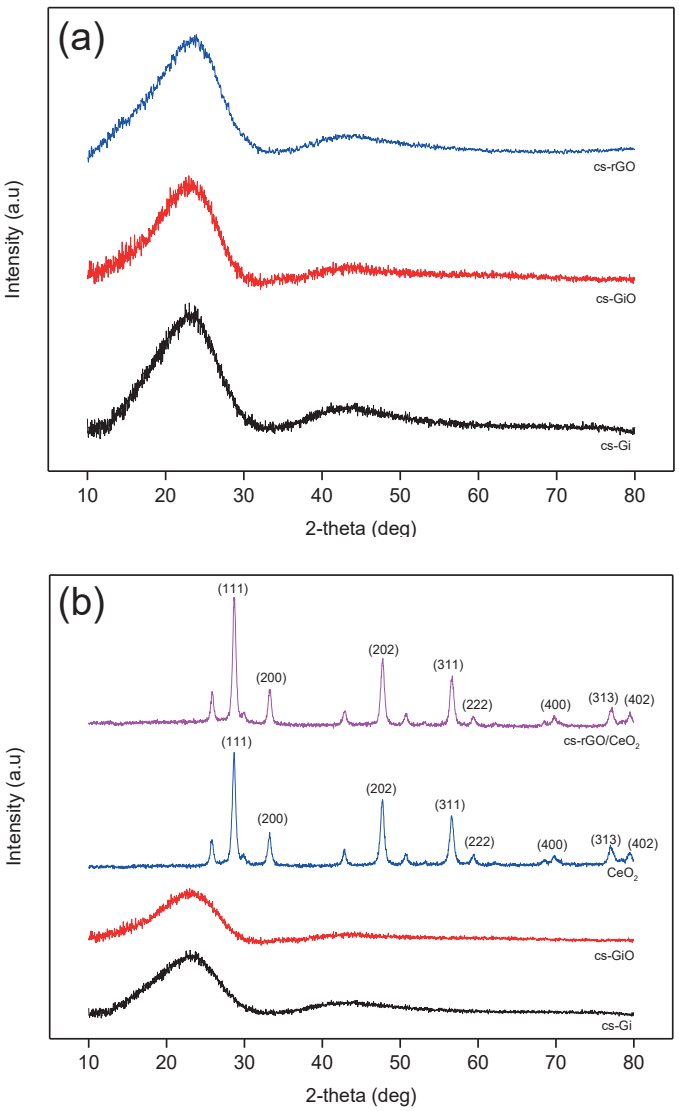


Figure 5: XRD pattern of (a) cs-Gi, cs-GiO, cs-rGO, and (b) cs-rGO/CeO_2

stretching associated with the sp^2 carbon network,[20] confirming the graphitic structure. The cs-Gi sample exhibits oxygen-containing groups such as O–H and C=O, originating from the precursor and thermal treatment.[28] After oxidation (cs-GiO), the intensity and variety of oxygen-containing groups increase, confirming successful functionalization during the modified Hummers process.[29] These groups facilitate exfoliation by increasing interlayer spacing.

Following hydrothermal reduction and CeO_2 decoration (Figure 7b), a decrease in oxygen-related functional groups is observed, indicating effective reduction and partial restoration of the sp^2 carbon network.[26] A characteristic band at 568 cm^{-1} corresponding to Ce–O vibrations confirms the presence of CeO_2.[23,27,32–33] The interaction between rGO and CeO_2 likely forms interfacial bonding, modifying the electronic structure of the composite.[34–35]

For the cs-rGO/CeO_2/epoxy composite (Figure 7c), characteristic peaks from both filler and matrix are observed. The retention of the C=C band confirms that the rGO structure is preserved after composite formation.[14] The absence of significant peak shifts suggests that the chemical structure of the filler remains stable. The interaction between filler and matrix is likely governed by interfacial bonding, promoting uniform dispersion.[36] From a functional perspective, the evolution of functional groups may influence EM wave absorption. Residual oxygen groups and interfacial features can contribute to polarization effects, while the restored sp^2 network may affect electrical conductivity. Together, these factors are expected to contribute to dielectric loss and EM wave attenuation.

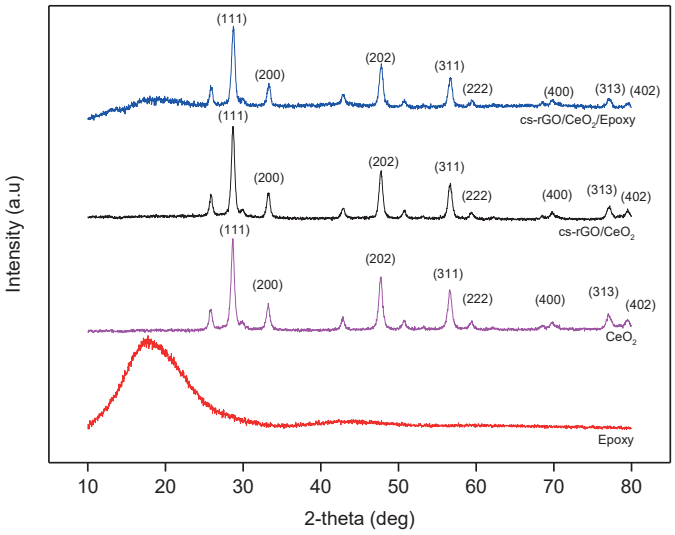


Figure 6: XRD pattern of cs-rGO/CeO_2/epoxy

Table 2: The value of D, d-spacing, and crystallinity for all samples

Samples	D (nm)	d-spacing (nm)	Crystallinity (%)
cs-Gi	-	0.376	76.16
cs-GiO	-	0.387	35.55
cs-rGO	-	0.371	24.90
cs-rGO/CeO_2	14.50	0.256	69.35
cs-rGO/CeO_2/epoxy	15.38	0.255	26.88

Microwave absorption properties of cs-rGO/CeO_2/epoxy composite

The microwave absorption performance of the cs-rGO/CeO_2/epoxy composite was evaluated using a vector network analyzer (VNA) in the X-band frequency range. The reflection loss (RL), derived from the S_{11} parameter, is widely used to assess electromagnetic (EM) wave absorption, where lower RL values indicate stronger absorption performance. The S_{11} parameter represents the reflection loss, while the S_{21} parameter corresponds to the insertion loss (IL) of the composite.[37–38] Both parameters are typically expressed in decibels (dB).

As shown in Figure 8a, the composite with a thickness of 1 mm exhibits a maximum RL of −7.72 dB at 9.77 GHz. Although the RL value is lower than those reported for similar graphene-based composites,[14–15] higher absorption performance is generally achieved at greater thicknesses (2–6 mm). Therefore, the present result indicates moderate absorption performance at a relatively low thickness, suggesting potential for lightweight absorber applications.

The observed absorption behavior can be attributed to dielectric loss and interfacial effects within the composite system. The rGO component provides conductive pathways, while the incorporation of CeO_2 introduces dielectric heterogeneity.[18] In addition, the rough surface morphology observed in SEM analysis may facilitate multiple scattering of incident EM waves, contributing to energy attenuation. The presence of CeO_2 is expected to alter the dielectric properties of the composite by introducing additional interfaces and structural heterogeneity, which may contribute to EM wave attenuation.[8,39] However, the relatively low RL value suggests that the absorption performance is not yet optimized, possibly due to the limited CeO_2 content and the lack of significant magnetic contributions.[40] The absence of detailed dielectric parameter analysis also limits a comprehensive understanding of the dominant absorption mechanisms. Therefore, while the observed structural and compositional features suggest a combined contribution to EM attenuation, further studies are required to clarify the underlying mechanisms.

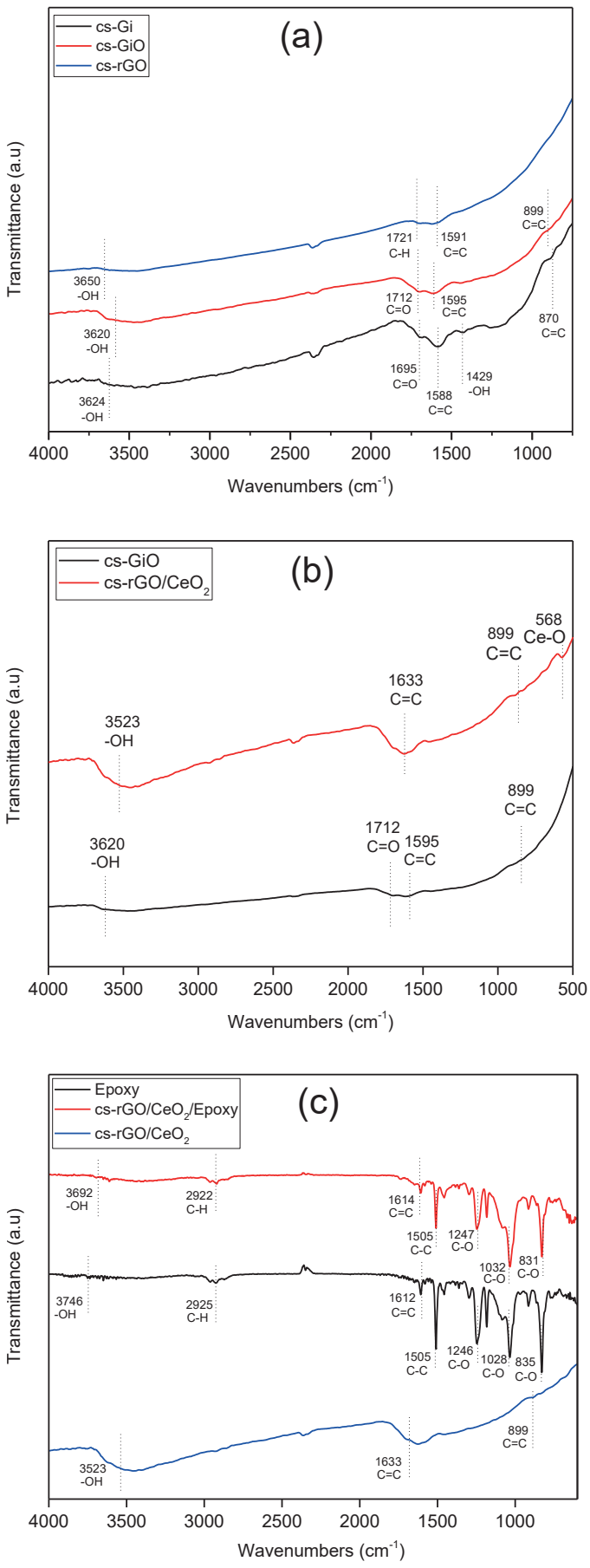


Figure 7: FT-IR spectra of (a) cs-Gi, cs-GiO, cs-rGO, (b) cs-rGO/CeO_2, (c) cs-rGO/CeO_2/epoxy

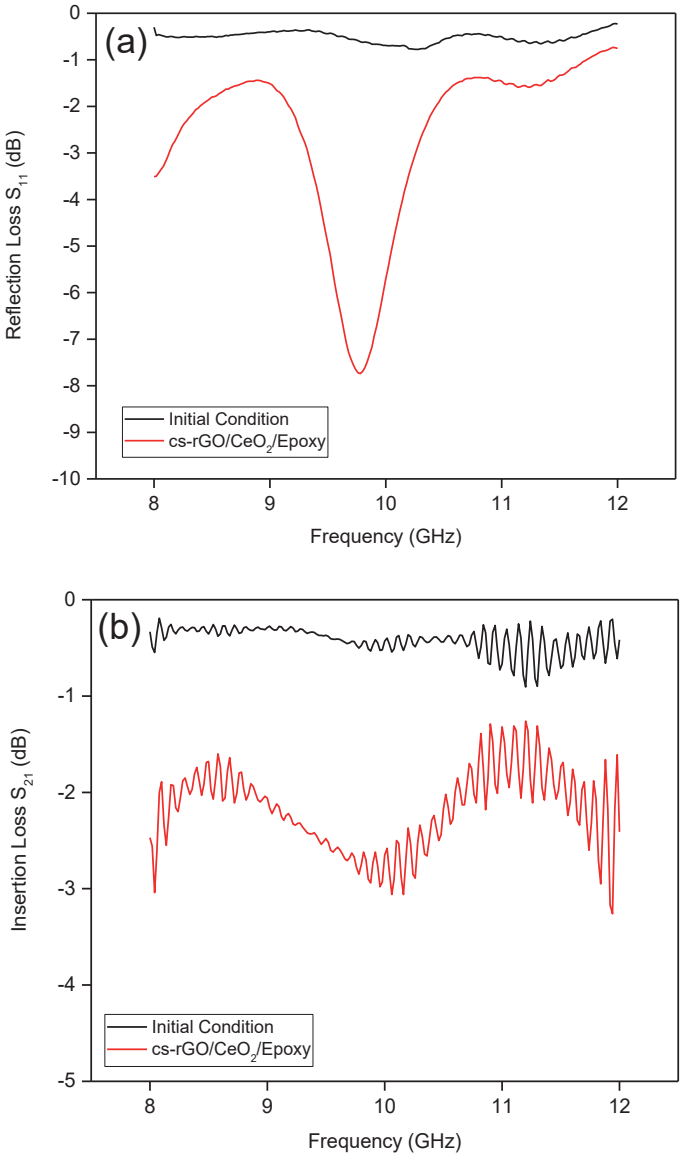


Figure 8: RL value (a) and IL value (b) of cs-rGO/CeO_2/epoxy

Further analysis based on the reflection coefficient (Γ) indicates that the composite exhibits approximately 16% reflected power and 84% transmitted power, suggesting that a substantial portion of the incident EM waves is not fully attenuated. This observation is consistent with the measured RL values. As reported in previous studies, materials exhibiting absorption levels above 70% are considered promising for further development.[38,41–42] Analysis of the transmission characteristics (S_{21} parameter) shows that the composite exhibits a maximum insertion loss of −1.26 dB at 11.20 GHz (Figure 8b). This relatively low attenuation indicates that part of the incident EM waves is transmitted through the material, further supporting the moderate absorption performance.[36]

As summarized in Table 4, the RL performance of composite materials depend on their composition, particularly the balance between dielectric and magnetic component.[16] In the present system, the absence of significant magnetic loss may limit overall absorption efficiency. Although each component of the cs-rGO/CeO_2/epoxy system exhibits relatively low RL values, the ability of the composite to achieve measurable absorption at a thickness of only 1 mm is notable. Thin absorbers are desirable for applications requiring lightweight and compact materials. Therefore, further optimization of composition, filler loading, and impedance matching is expected to improve the microwave absorption performance of the cs-rGO/CeO_2/epoxy composite.

Table 3: List of identified wavenumbers (in cm^{-1}) of all samples by FT-IR analysis

Materials	–OH Alcohol	–OH Carb. acid	C=O Carbonyl	C–O Epoxy	C=C Cyclic Alkene	C–C Aromatic	C–H Alkene	C–H Aromatic	Ce–O
cs-Gi	3624	1429	1695	-	1588, 870	-	-	-	-
cs-GiO	3620	-	1712	-	1595, 899	-	-	-	-
cs-rGO	3650	-	-	-	1591	-	-	1721	-
cs-rGO/CeO_2	3523	-	-	-	1633, 899	-	-	-	568
Epoxy	3746	-	-	1246, 1028, 835	1612	1505	2925	-	-
cs-rGO/CeO_2/epoxy	3692	-	-	1247, 1032, 831	1614	1505	2922	-	568

Table 4: Comparison of RL_{max} value for carbon-based RAM

Samples	Thickness (mm)	Frequency (GHz)	RL_{max} (dB)	Ref.
rGO (obtained from natural graphite flakes)	2	12	-5.10	(13)
CeO_2	2	15.84	-0.63	(16)
Epoxy	4	10	-0.21	(14)
rGO/Epoxy	6	12	-25.74	(14)
CeO_2-rGO	2	4.50	-45.90	(16)
Fe-Cr/rGO	5	6.86	-10.65	(32)
cs-rGO/CeO_2/epoxy	1	9.77	-7.72	This research

CONCLUSION

In this study, a cerium(IV) oxide (CeO_2)-decorated coconut shell-derived reduced graphene oxide (cs-rGO) composite dispersed in an epoxy matrix was synthesized via a modified Hummers method followed by hydrothermal reduction. Structural and chemical characterization confirmed the reduction of graphene oxide, the incorporation of CeO_2 nanoparticles, and the homogeneous dispersion of the filler within the polymer matrix. The combination of rGO and CeO_2 forms a heterogeneous structure that promotes dielectric loss and interfacial polarization, while the rough surface morphology facilitates multiple scattering of EM waves. The composite exhibits a maximum reflection loss of −7.72 dB at 9.77 GHz at a thickness of 1 mm, indicating moderate microwave absorption performance at low thickness. Although the absorption performance is lower than that reported for thicker or more optimized systems, the ability to achieve measurable attenuation at a low thickness highlights the potential of this material as a lightweight radar-absorbing material. Further optimization, particularly in terms of CeO_2 loading, dispersion quality, and impedance matching, may improve the overall absorption efficiency of the composite.

SUPPLEMENTARY INFORMATION

This manuscript does not have Supplementary Information. All the data is presented in the article.

ACKNOWLEDGEMENT

The authors highly acknowledge the financial support provided by the LPDP-BRIN trough RIIM VII program, agreement number 41/IV/KS/02/2025 and PKS/19/II/2025/UNHANRI.

CREDIT AUTHORSHIP CONTRIBUTION STATEMENT

Patricya Inggrid Wilhelmina Bolilanga: Conceptualization, Investigation, Methodology, Writing–original draft, review & editing. Rahmat Basuki: Supervision, Methodology, Writing–review. Nugroho Adi Sasongko and Gunaryo: Supervision, Formal Analysis. Arief Budi Santiko: Supervision, Formal Analysis. Yusuf Bramastya Apriliyanto: Supervision, Methodology.

DECLARATION OF COMPETING OR FINANCIAL INTERESTS

The authors declare that have no financial interests or personal relationships that could have appeared to influence the work reported in this paper.

DECLARATION OF GENERATIVE AI AND AI-ASSISTED TECHNOLOGIES

The authors declare that, during the preparation of this manuscript, AI-assisted tools were solely for language and grammar revision. All outputs were critically reviewed and edited by the authors, who assume full responsibility for the content.

AUTHORS ORCIDS

Patricya Inggrid Wilhelmina Bolilanga: https://orcid.org/0009-0000-7140-9231
Rahmat Basuki: https://orcid.org/0000-0002-3117-2740
Nugroho Adi Sasongko: https://orcid.org/0000-0002-6546-1348
Yusuf Bramastya Apriliyanto: https://orcid.org/0000-0003-0683-8456
Arief Budi Santiko: https://orcid.org/0009-0000-8249-7476
Gunaryo Gunaryo: https://orcid.org/0009-0008-1510-2110

REFERENCES

1. Shinde DD, Babu V, Khandal S V. A review on types of radar absorbing materials. Shanlax Int J Manag. 2022;9(S1-Mar):122–127. https://doi.org/10.34293/management.v9iS1-Mar.4901.
2. Das S, Nayak GC, Sahu SK, Routray PC, Roy AK, Baskey H. Microwave absorption properties of double-layer radar absorbing materials based on doped Barium hexaferrite/TiO_2/conducting Carbon Black. J Eng. 2014;2014:1–5. https://doi.org/10.1155/2014/468313.
3. Esmaeili S, Sedghi H. Radar absorbing materials mechanism and effective parameters in behavior improving. Int J Recent Technol Eng. 2019;3878(1):1955–1959.
4. Ruiz-Perez F, López-Estrada SM, Tolentino-Hernández RV, Caballero-Briones F. Carbon-based radar absorbing materials: A critical review. J Sci Adv Mater Devices. 2022;7(3):100454. https://doi.org/10.1016/j.jsamd.2022.100454.
5. Aytaç A, İpek H, Aztekin K, Çanakçı B. A review of the radar absorber material and structures. Sci J Mil Univ L Forces. 2020;198(4):931–946. https://doi.org/10.5604/01.3001.0014.6064.
6. Wang Y, Li T, Zhao L, Hu Z, Gu Y. Research progress on nanostructured radar absorbing materials. Energy Power Eng. 2011;3(4):580–584. https://doi.org/10.4236/epe.2011.34072.
7. Shen Z, Xing H, Wang H, Jia H, Liu Y, Chen A, Yang P. Synthesis and enhanced electromagnetic absorption properties of Co-doped CeO_2/rGO nanocomposites. J Alloys Compd. 2018;753:28–34. https://doi.org/10.1016/j.jallcom.2018.04.195.
8. Wang S, Gao F, Zhao Y, Liu N, Tan T, Wang X. Two-Dimensional CeO_2/rGO composite-modified separator for Lithium/Sulfur batteries. Nanoscale Res Lett. 2018;13(1):377. https://doi.org/10.1186/s11671-018-2798-5.
9. Abbas Q, Shinde PA, Abdelkareem MA, Alami AH, Mirzaeian M, Yadav A, et al. Graphene synthesis techniques and environmental applications. Materials (Basel). 2022;15(21):7804. https://doi.org/10.3390/ma15217804.
10. Lesiak B, Trykowski G, Tóth J, Biniak S, Kövér L, Rangam N, Stobinski L,

Malolepszy A. Chemical and structural properties of reduced graphene oxide—dependence on the reducing agent. J Mater Sci. 2021;56(5):3738–3754. https://doi.org/10.1007/s10853-020-05461-1.

11. Dideikin AT, Vul' AY. Graphene oxide and derivatives: the place in graphene family. Front Phys (Lausanne). 2019;6(JAN):149. https://doi.org/10.3389/fphy.2018.00149.
12. Balci O, Polat EO, Kakenov N, Kocabas C. Graphene-enabled electrically switchable radar-absorbing surfaces. Nat Commun. 2015;6(1):6628. https://doi.org/10.1038/ncomms7628.
13. Yin Q, Xing H, Shu R, Ji X, Tan D, Gan Y. Enhanced microwave absorption properties of CeO_2 nanoparticles supported on Reduced Graphene Oxide. Nano. 2016;11(5):1650058. https://doi.org/10.1142/S1793292016500582.
14. Ahmad AF, Ab Aziz S, Abbas Z, Obaiys SJ, Khamis AM, Hussain IR, Zaid MHM. Preparation of a chemically Reduced Graphene Oxide reinforced Epoxy Resin Polymer as a composite for electromagnetic interference shielding and microwave-absorbing applications. Polymers (Basel). 2018;10(11):1180. https://doi.org/10.3390/polym10111180.
15. Sujiono EH, Zurnansyah, Zabrian D, Dahlan MY, Amin BD, Samnur, Agus J. Graphene oxide based coconut shell waste: synthesis by modified Hummers method and characterization. Heliyon. 2020;6(8):e04568. https://doi.org/10.1016/j.heliyon.2020.e04568.
16. Wang Z, Zhao P, He D, Cheng Y, Liao L, Li S, Luo Y, Peng Z, Li P. Cerium oxide immobilized Reduced Graphene Oxide hybrids with excellent microwave absorbing performance. Phys Chem Chem Phys. 2018;20(20):14155–14165. https://doi.org/10.1039/C8CP00160J.
17. Shalaby A, Nihtianova D, Markov P, Staneva AD, Iordanova RS, Dimitriev YB. Structural analysis of Reduced Graphene Oxide by transmission electron microscopy. Bulg Chem Commun. 2015;47(1):291–295.
18. Ban GD, Liu ZH, Ye ST, Yang HB, Tao R, Luo P. Microwave absorption properties of Carbon Fiber radar absorbing coatings prepared by water-based technologies. RSC Adv. 2017;7(43):26658–26664. https://doi.org/10.1039/C7RA02631E.
19. Zhang G, Chen Y, Chen Y, Guo H. Activated biomass carbon made from bamboo as electrode material for supercapacitors. Mater Res Bull. 2018;102:391–398. https://doi.org/10.1016/j.materresbull.2018.03.006.
20. Olowojoba GB, Kopsidas S, Eslava S, Gutierrez ES, Kinloch AJ, Mattevi C, Rocha VG, Taylor AC. A facile way to produce Epoxy nanocomposites having excellent thermal conductivity with low contents of Reduced Graphene Oxide. J Mater Sci. 2017;52(12):7323–7344. https://doi.org/10.1007/s10853-017-0969-x.
21. Farahmandjou M, Farahmandjou M, Zarinkamar M, Firoozabadi TP. Synthesis of Cerium Oxide (CeO_2) nanoparticles using simple CO-precipitation method. Rev Mex Fis. 2016;62(October):496–499.
22. Xue J, Wu C, Du X, Ma W, Wen K, Huang S, Liu Y, Liu Y, Zhao G. Preparation and properties of functional particle Fe_3O_4-rGO and its modified fiber/epoxy composite for high-performance microwave absorption structure. Mater Res Express. 2020;7(4):045303. https://doi.org/10.1088/2053-1591/ab8257.
23. Thakur A, Kumar S, Rangra VS. Synthesis of Reduced Graphene Oxide (rGO) via chemical reduction. AIP Conf Proc. 2015;1661:080032. https://doi.org/10.1063/1.4915423.
24. Tarcan R, Todor-Boer O, Petrovai I, Leordean C, Astilean S, Botiz I. Reduced Graphene Oxide today. J Mater Chem C Mater Opt Electron Devices. 2020;8(4):1198–1224. https://doi.org/10.1039/C9TC04916A.
25. Gutiérrez-Portocarrero S, Roquero P, Becerril-González M, Zúñiga-Franco D. Study of structural defects on Reduced Graphite Oxide generated by different reductants. Diamond Related Materials. 2019;92:219–227. https://doi.org/10.1016/j.diamond.2019.01.001.
26. Rukman NK, Jannatin M, Supriyanto G, Fahmi MZ, Ibrahim WAW. GO-Fe_3O_4 Nanocomposite from coconut shell: synthesis and characterization. IOP Conf Ser Earth Environ Sci. 2019;217:012008. https://doi.org/10.1088/1755-1315/217/1/012008.
27. Cao N, Zhang Y. Study of Reduced Graphene Oxide Preparation by Hummers' Method and Related Characterization. J Nanomater. 2015;2015(1):168125. https://doi.org/10.1155/2015/168125.
28. Zainuddin MF, Nik Raikhan NH, Othman NH, Abdullah WFH. Synthesis of Reduced Graphene Oxide (rGO) using different treatments of Graphene Oxide (GO). IOP Conf Ser Mater Sci Eng. 2018;358:012046. https://doi.org/10.1088/1757-899X/358/1/012046.
29. Taufantri Y, Irdhawati I, Asih IARA. Sintesis dan karakterisasi Grafena dengan metode Reduksi Grafit Oksida menggunakan pereduksi Zn. J Kim Val. 2016;2(1):17–23. https://doi.org/10.15408/jkv.v2i1.2233.
30. Bandara N, Esparza Y, Wu J. Graphite Oxide improves adhesion and water resistance of Canola Protein-Graphite Oxide Hybrid Adhesive. Sci Rep. 2017;7(1):11538. https://doi.org/10.1038/s41598-017-11966-8.
31. Mas'udah KW, Taufiq A, Sunaryono S. Sunaryono. The potential of corncobs in producing reduced graphene oxide as a semiconductor material. J Eng Technol Sci. 2022;54(2):220201. https://doi.org/10.5614/j.eng.technol.sci.2022.54.2.1.
32. Gharagozloo Bahrami AB, Bahrami SH, Saber-Samandari S, Kowsari E. New functional Graphene Oxide based on transition metal complex (Cr/Fe) as wave absorber. J Mater Res Technol. 2022;20:3683–3696. https://doi.org/10.1016/j.jmrt.2022.08.061.
33. Manoratne CH, Rosa SRD, Kottegoda IRM. XRD-HTA, UV Visible, FTIR and SEM Interpretation of Reduced Graphene Oxide synthesized from high purity vein Graphite. Mater Sci Res India. 2017;14(1):19–30. https://doi.org/10.13005/msri/140104.
34. Verma R, Samdarshi SK. In situ decorated optimized CeO_2 on Reduced Graphene Oxide with enhanced adsorptivity and visible light photocatalytic stability and reusability., Journal of Physical Chemistry C. 2016;120:22281–22290. https://doi.org/10.1021/acs.jpcc.6b04493.
35. Dezfuli AS, Ganjali MR, Norouzi P, Faridbod F. Facile sonochemical synthesis and electrochemical investigation of Ceria/Graphene nanocomposites. J Mater Chem B. 2015;3(11):2362–2370. https://doi.org/10.1039/C4TB01847H.
36. Strankowski M, Włodarczyk D, Piszczyk Ł, Strankowska J. Polyurethane nanocomposites containing Reduced Graphene Oxide, FTIR, Raman, and XRD Studies. J Spectrosc. 2016;2016:1–6. https://doi.org/10.1155/2016/7520741.
37. Hasan MZ, Wijanto H, Sigit V. Bandpass filter mikrostrip untuk radar cuaca s-band menggunakan meander loop dual resonator. E-Proceeding Eng. 2019;6(2):3628–3635.
38. Guo Y, Song X, Ma S, Qi Y, Yuan X, Fan H. Preparation of bunched CeO_2 and study on microwave absorbing properties with MWCNTs binary composite. Particuology. 2023;73:95–102. https://doi.org/10.1016/j.partic.2022.04.002.
39. Khan S, Bari P, Mishra S. Effect of chemically Reduced Graphene Oxide on mechanical and thermal properties of Epoxy nano composites. J Mater Sci Nanotechnol. 2019;7(2):1–9.
40. Xu C, Shi X, Ji A, Shi L, Zhou C, Cui Y. Fabrication and characteristics of Reduced Graphene Oxide produced with different green reductants. PLoS One. 2015;10(12):e0144842. https://doi.org/10.1371/journal.pone.0144842.
41. Mittal G, Lee SW, Rhee KY. Reduced Graphene Oxide coating on basalt fabric using electrophoretic deposition and its role in the mechanical and tribological performance of Epoxy/Basalt fiber composites. Nanotechnol Rev. 2021;10(1):1383–1394. https://doi.org/10.1515/ntrev-2021-0091.
42. Chan YL, You KY, Mayzan MZH, Jusoh MA, Abas Z, Esa F. Investigation into return loss characteristic of graphene oxide/zinc ferrite/epoxy composite at X-band frequency. J Appl Sci Eng. 2020;23(4):593–602.